Carbohydrate Polymers 82 (2010) 733–741

Contents lists available at ScienceDirect

Carbohydrate Polymers

journal homepage: www.elsevier.com/locate/carbpol

Synergistic interaction of Locust Bean Gum and Xanthan investigated by rheology and light scattering

Chiara Sandolo[a], Donatella Bulone[b], Maria R. Mangione[b], Silvia Margheritelli[a], Chiara Di Meo[a], Franco Alhaique[a], Pietro Matricardi[a], Tommasina Coviello[a,*]

[a] Department of Drug Chemistry and Technologies, Faculty of Pharmacy, "Sapienza", University of Rome, 00185 Rome, Italy
[b] Institute of Biophysics at Palermo Italian National Research Council Via Ugo La Malfa, 153 90146 Palermo, Italy

ARTICLE INFO

Article history:
Received 26 April 2010
Received in revised form 20 May 2010
Accepted 21 May 2010
Available online 31 May 2010

Keywords:
Polysaccharides
Synergistic interactions
Hydrogels
Rheology
Light scattering
Gel point

ABSTRACT

The use of synergistic interactions between polysaccharides can represent an important approach for the preparation of physical networks with a wide range of industrial applications, such as in the food and biomedical fields. Locust Bean Gum and Xanthan, two biocompatible polymers, are able to form gels when mixed together. A detailed study was carried out on three samples, prepared at different weight ratios and two temperatures, by means of light scattering and rheological techniques. The solid-like character of each sample was evaluated by measurements of the viscoelastic spectrum and intensity autocorrelation function. The contribution of fast and slow fluctuations to the static light scattered intensity was also evaluated at different angles. The power law exponents for the sol–gel transitions were estimated together with the fractal dimensions. The scattering results were found in good agreement with the mechanical ones in revealing a strong dependence of the structural properties of the different samples on their preparation conditions. Indeed, results show that a fine tuning of the properties of the mixed gels is possible through the change of the temperature preparation and/or the polymer weight ratio.

1. Introduction

Binary mixtures of certain polysaccharides often exhibit unexpected synergistic interactions, e.g., the mixture may gel under conditions where the individual components are non-gelling. Striking example of this behaviour occurs when the bacterial polysaccharide Xanthan gum (Scheme 1) is mixed with some plant galactomannans (Morris, 1990). It is well known that the synergistic gelation occurs by direct binding between the two polymers and not by thermodynamic incompatibility. Furthermore, X-ray diffraction pattern obtained from fibres prepared from the synergistic gel, are new patterns and not the simple sum of the diffraction patterns of the component polysaccharides (Cairns, Miles, Morris, & Brownsey, 1988). In particular, Xanthan and Locust Bean Gum (LBG) (Scheme 1), when mixed together, give a network whose strength depends on the temperature preparation and on the weight ratio between the two components. A wide debate is still open in elucidating the actual mechanism leading to the gel formation and, during the past decades, several models have been proposed (Lundin & Hermansson, 1995; Richter, Boyko, Matzker, & Schröter, 2004; Richter, Brand, & Berger, 2005; Wang, Wang, & Sun, 2002; Zhan, Ridout, Brownsey, & Morris, 1993). It is acquired that the presence of the acetyl substituents on the Xanthan chains (Ojinnaka, Brownsey, Morris, & Morris, 1998; Wang et al., 2002) as well as the branching degree of the galactomannan are crucial for gel formation (an increase of the number of galactose units hinders gel formation (Dea, Clark, & McCleary, 1986)).

The possibility to modulate the mechanical properties of the gel by varying the relative amount of the two polymers and taking also into account the different conformations assumed by the Xanthan chains in distilled water at 25 °C (described in terms of a double-helix ordered structure) and at $T > 45$ °C (random coil conformation) (Coviello, Kajiwara, Burchard, Dentini, & Crescenzi, 1986; Hacche, Washington, & Brant, 1987) appears to be particularly interesting. The temperature at which the helix–coil transition occurs, T_m, deeply depends on several factors (ionic strength, content of pyruvate and acetate minor components) and therefore for the "hot samples" preparation a rather high temperature, $T = 75$ °C, was adopted. In the present work a comparison among three samples prepared at different weight ratios and two temperatures is reported: rheological characterization and light scattering techniques were applied. Morphological features of the samples, acquired by means of SEM spectroscopy, are also given.

The importance of a study on this binary mixture is also supported by the fact that these polymers (both individually and mixed together) are already widely used in food industry

* Corresponding author. Tel.: +39 06 49913557; fax: +39 06 49913133.
E-mail address: tommasina.coviello@uniroma1.it (T. Coviello).

0144-8617/$ – see front matter © 2010 Elsevier Ltd. All rights reserved.
doi:10.1016/j.carbpol.2010.05.044

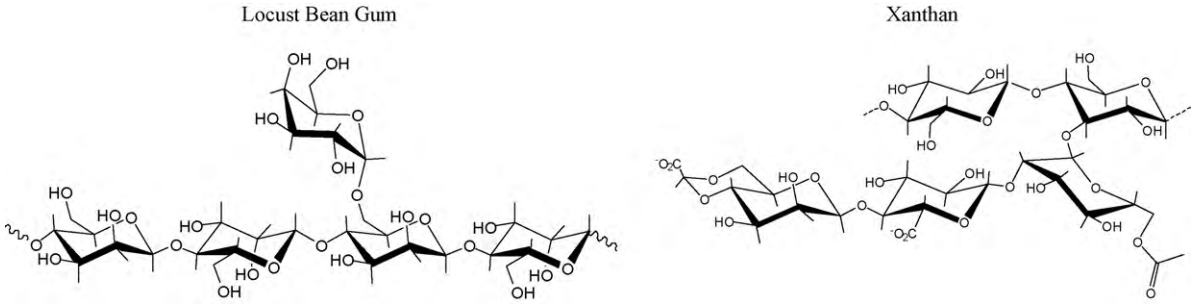

Scheme 1. Repeating units of LBG (left) and xanthan (right).

(Dolz, Hernández, Delegido, Alfaro, & Muñoz, 2007; Mandala, Kapetanakou, & Kostaropoulos, 2008; Pedersen, 1980; Ramírez, Barrera, Morales, & Vázquez, 2002; Sahin & Ozdemir, 2004; Secouard, Malhiac, Grisel, & Decroix, 2003). Furthermore, it must be pointed out that the single polymers are already used as excipients in tablet formulations, and the LBG/Xanthan gels have been proposed in pharmaceutical applications for slow release purposes (Baichwal, 2004; Fadden, Kulkarni, & Sorg, 2004; Mannion, Melia, Mitchell, Harding, & Green, 1991; Rolf, 2003; Sugden, 1989; Ughini, Andreazza, Ganter, & Bresolin, 2004; Venkataraju, Gowda, Rajesh, & Shivakumar, 2008). The biocompatibility of the two polysaccharides, together with their peculiar synergic behaviour, can still offer new interesting applications. In this sense, even more significant appears to be any attempt to elucidate the molecular structure and the spectroscopic characteristics of these mixed gels in order to improve and to better modulate their potential uses.

2. Materials and methods

2.1. Materials

Locust Bean Gum (LBG), from *Ceratonia Campestris*, was provided by Carbomer (USA). The ratio between mannose and galactose, was estimated by means of ^{1}H NMR (carried out at 70 °C with a Brucker AVANCE AQS 600 spectrometer, operating at 600.13 MHz) and an M/G value of ∼3.4 was found. The molecular weight (M_w) of LBG, 5.0×10^5, was estimated from the usual Zimm plot analysis of static light scattering measurements carried out at 25 °C in 0.1 M NaCl aqueous solutions of sterilized LBG. The estimated radius of gyration was R_g = 102 nm and the second virial coefficient $A_2 = -3.21 \times 10^{-4}$ cm^3 mol/g^2. Procedure details are given in the literature (Coviello et al., 1986).

Xanthan Gum, from *Xanthomonas campestris*, was provided by Fluka (Italy). For each repeating unit, 1.6 acetate and 2.7 pyruvate groups were estimated by ^{1}H NMR measurements (carried out at 85 °C with a Brucker AVANCE AQS 600 spectrometer, operating at 600.13 MHz). The molecular weight (M_w) of Xanthan, 1.25×10^6, was obtained by means of static light scattering measurements, carried out at 25 °C in 0.1 M NaCl aqueous solutions of sterilized Xanthan, and reported according to the classical Zimm plot representation. The estimated radius of gyration was R_g = 140 nm and the second virial coefficient $A_2 = +6.09 \times 10^{-4}$ cm^3 mol/g^2.

The two polysaccharides were used after sterilization, centrifugation and purification. A given amount of Xanthan, sodium salt, (polymer concentration, c_p = 0.5%, w/v) was dissolved in distilled water, under magnetic and mechanical stirring, at room temperature for 48 h, while LBG (c_p = 0.5%, w/v) was dispersed in distilled water, under magnetic and mechanical stirring, at 80 °C for 24 h and at room temperature for 24 additional hours (Kok, Hill, & Mitchell, 1999). The obtained solutions were autoclaved at 121 °C for 20 min and then centrifuged at 8000 rpm for 15 min at 25 °C. The supernatant solutions (the polymer weight loss was ∼15% in the case of Xanthan and ∼30% for LBG) were then exhaustively dialyzed at 4 °C against distilled water using dialysis membranes with a cut-off 12,000–14,000. In order to convert the Xanthan polymer in the sodium form, NaOH 0.2 N was added to the dialyzed solution up to pH = 7.0. Finally, the samples were freeze-dried and stored in a desiccator until use.

All other products and reagents were of analytical grade.

2.2. LBG/Xanthan hydrogel preparations

The LBG/Xanthan hydrogels were prepared by mixing appropriate amounts of LBG and Xanthan solutions (c_p = 0.125%, w/v) previously autoclaved at 121 °C for 20 min and filtered through cellulose nitrate membranes with pore sizes of 8 and 1.2 μm in sequence. It must be pointed out that the Xanthan chains undergo an order–disorder transition during autoclaving and therefore a renaturated state (where not necessarily perfect double-strands are formed) should be considered in the subsequent interactions with the LBG chains. Different aliquots of the two polymer solutions were mixed for 15 min at 75 °C ("hot gelation") (where the Xanthan chains adopt a coil conformation ($T > T_m$)) or at room temperature ("cold gelation") (where the Xanthan chains are in double helix conformation ($T < T_m$)), leading to samples with final different weight ratios. The "hot samples", after heating at 75 °C for 15 min, were left to slowly cool down in the switched off thermostatted bath, until room temperature was reached. Three samples were prepared, namely 1:1 (50% of both, LBG and Xanthan solutions), 1:3 (25% of LBG solution and 75% of Xanthan solution), and 1:9 (10% of LBG solution and 90% of Xanthan solution).

2.3. Rheological characterization

The rheological characterization of the LBG/Xanthan gels was performed by means of a controlled stress rheometer, Haake RheoStress RS300 model, with a Thermo Haake DC50 water bath; a grained plate-plate device (Haake PP35 T_I: diameter = 35 mm; gap between plates = 1 mm) was used in order to reduce the extent of the wall slippage phenomena (Lapasin & Pricl, 1995). Rheological properties were studied with oscillatory experiments; mechanical spectra were recorded in the frequency range 0.001–10 Hz. The linear viscoelastic region was assessed, at 1 Hz, by stress sweep experiments; a constant deformations, γ = 0.01, was used. All the samples were analyzed at 25 ± 1 °C, 1 day and 6 days after the mixing of the two polymer solutions.

2.4. Light scattering

Each sample was placed into a thermostatted cell compartment of a Brookhaven Instruments BI200-SM goniometer. The temperature was controlled to within 0.1 °C using a thermostatted recirculating bath. The light scattered intensity and time autocorrelation function (TCF) were measured by using a

Brookhaven BI-9000 correlator and a 100 mW Ar laser (Melles Griot) tuned at $\lambda = 514.5$ nm or a 50 mW He–Ne tuned at $\lambda = 632.8$ nm. Measurements were taken at different scattering vector $q = 4\pi n\lambda_0^{-1} \sin(\theta/2)$, where n is the refractive index of the solution, λ_0 is the wavelength of the incident light, and θ is the scattering angle. To overcome the non-ergodicity, typical of gelled systems (Pusey & van Megen, 1989; Rodd, Dunstan, Boger, Schmidt, & Burchard, 2001), the measurements were carried out by collecting the signal over different regions of the specimen, automatically scanned by means of a motor-driven cell holder. In dynamic light scattering (DLS) experiments the correlator operated in the multi-τ mode. About 150 measurements, lasting 7 min each, were taken over different sample positions; the intensity autocorrelation function was then obtained by their sum normalized by the square of the total photon number. The average scattered intensity factor and its dependence on q-vector were obtained by collecting the signal over large scattering volumes while the samples were continuously rotating. Static light scattering data were corrected for the background scattering of the solvent and normalized by using toluene as calibration liquid. The static light scattered intensity was also studied in terms of fluctuant and static components (Barthès, Bulone, Manno, Martorana, & San Biagio, 2007; Manno, Bulone, Martorana, & San Biagio, 2004). For this purpose about 700 intensity values were collected over different sample positions on a scattering volume corresponding to a single speckle. The integration time (T_I) for a single measurement was 1 s.

2.5. Data analysis

Data distribution of the scattered intensity was analyzed with an expression (Barthès et al., 2007; Manno et al., 2004) derived by extending the Pusey and van Megen theory for non-ergodic media to the case of no completely frozen-in systems. Indeed, the core of this expression is the ratio between the coherence time of the scattering radiation and the integration time T_I of the measurement of the scattered intensity. As in the Pusey and van Megen approach, it was assumed that the total scattered field E is the sum of a fast-fluctuating field E_F due to small-size objects with an average intensity I_F and a coherence time $\tau_F < T_I$, and a slowly decaying field E_S due to large-size slowly diffusing objects, with an average intensity I_S and a coherence time $\tau_S > T_I$. By taking into account the ratio $N = \tau_F/T_I$, it was shown that the total time-integrated intensity is given by two statistically independent contributions: an exponentially slow contribution with average $\bar{I}_{NG} = \bar{I}_S + 2\bar{I}_F/N$, and a Gaussian distributed fast contribution with average $\bar{I}_G = \bar{I}_F - 2\bar{I}_F/N$ and variance $\sigma^2 = \bar{I}_G^2/N$. The expression for intensity distribution function is:

$$P(I_{T_I}) = \frac{1}{\bar{I}_G}\exp\left\{-\frac{\left[I-\bar{I}_G\right]}{\bar{I}_{NG}}\right\} \times \left[\operatorname{erf}\left(\frac{I}{\sigma\sqrt{2}} - \frac{\bar{I}_G\bar{I}_{NG}+\sigma^2}{\bar{I}_{NG}\sigma\sqrt{2}}\right) + \operatorname{erf}\left(\frac{\bar{I}_G\bar{I}_{NG}+\sigma^2}{\bar{I}_{NG}\sigma\sqrt{2}}\right)\right] \times \frac{1}{2}\exp\left(\frac{\sigma^2}{2\bar{I}_{NG}}\right) C \quad (1)$$

where $\operatorname{erf}(x) = 2\sqrt{\pi}\int_0^x e^{-t^2}dt$ is the error function and $C \approx 1$ is a normalization constant: $C = 1/2[1 + \operatorname{erf}(I_G/\sigma\sqrt{2})]$.

The expression is correct to the first order in τ_F/T_I and allows to distinguish between a fast fluctuating and a slowly relaxing contribution even when their time scales are not completely separated.

2.6. Scanning electron microscopy (SEM)

The SEM images were obtained using a FEI Quanta 400 FEG apparatus. Freeze-dried hydrogels were mounted on appropriate stubs and examined under vacuum (50 Pa), with no need of the gold coating technique, at an accelerating voltage of 15 kV. All images were acquired digitally using xTmicroscope Control software and at 800× magnification.

3. Results and discussion

3.1. Rheological investigations

The mechanical spectra of the LBG/Xanthan samples, prepared at different weight ratios in "hot" and "cold conditions" recorded at 25 °C 1 day after and 6 days after the mixing of the two polymer solutions (in the meanwhile the samples were kept at a constant temperature of 25 °C), are shown in Fig. 1.

It is well known that both polymers, alone, are not capable to form gels, while, when mixed in appropriate amounts, a three-dimensional network is formed. It is evident that, when the polymer solutions are mixed in "cold conditions" the degree of entanglements and the number of effective physical cross-links is deeply dependent on the weight ratio considered (see Fig. 1). If Xanthan is the main component of the mixture (1:9), then the typical solution behaviour is observed: the loss modulus is always higher than the storage modulus and both show a strong dependence on the applied frequency. If the amount of Xanthan is reduced, but still predominant in comparison with LBG (1:3), the characteristic gel point is observed. At the gel point the G' and G'' moduli overlap and increase together, showing the typical power law behaviour (see below). Further decrease of the Xanthan percentage in the mixture (1:1) leads to the formation of a gel, i.e., in the whole range of explored frequencies (ca. four decades), G' is always higher than G''. It must be underlined that, for an appropriate comparison with LS experiments, the used polymer concentration is quite low ($c_p = 0.125\%$). As a consequence the formed gel is a weak network: the difference between G' and G'' values is less than a factor ten. Furthermore, the complete gel formation does not occur instantaneously: consequently the time evolution of the moduli was followed and the measurements were carried out also after 6 days (see Fig. 2(A–C)). For the 1:9 and 1:1 ratios an increase of G' is observed. For the 1:1 ratio the frequency dependence remains the same but the difference between the two moduli increases with time indicating an increase of the number of the physically active bonds. A similar behaviour is detected for the 1:9 ratio: the frequency dependence does not change with time, the G'' values are almost the same at 1 and 6 days while an increase with time is observed for G'. Nevertheless this increase does not change the nature of the system that shows always a solution behaviour ($G' < G''$).

On the other side, when the two polymer solutions are mixed in "hot conditions", remarkable differences are registered in the mechanical spectra (Figs. 1(C and D) and 2(D–F)). All absolute values of the moduli are higher than those of the "cold samples" indicating that, when Xanthan is in a disordered conformation, a more entangled network with a higher number of effective cross-links can be formed in the presence of LBG (see Fig. 2). For the sample with the 1:1 weight ratio, after 1 day, a gel is already formed, although a slight dependence from the frequency can be observed for both moduli (Fig. 2(D)). After 6 days, an almost independence on the frequency is monitored (Fig. 2(D)): this is an indication that the network evolves and more effective physical cross-links are formed with time, which contribute to the elastic modulus.

Also for the network prepared at 1:9 ratio in "hot conditions", an evolution is observed (Fig. 2(F)); but, while for the "hot sample" a gel point occurs already after 1 day (Fig. 2(F)) (similar spectra were

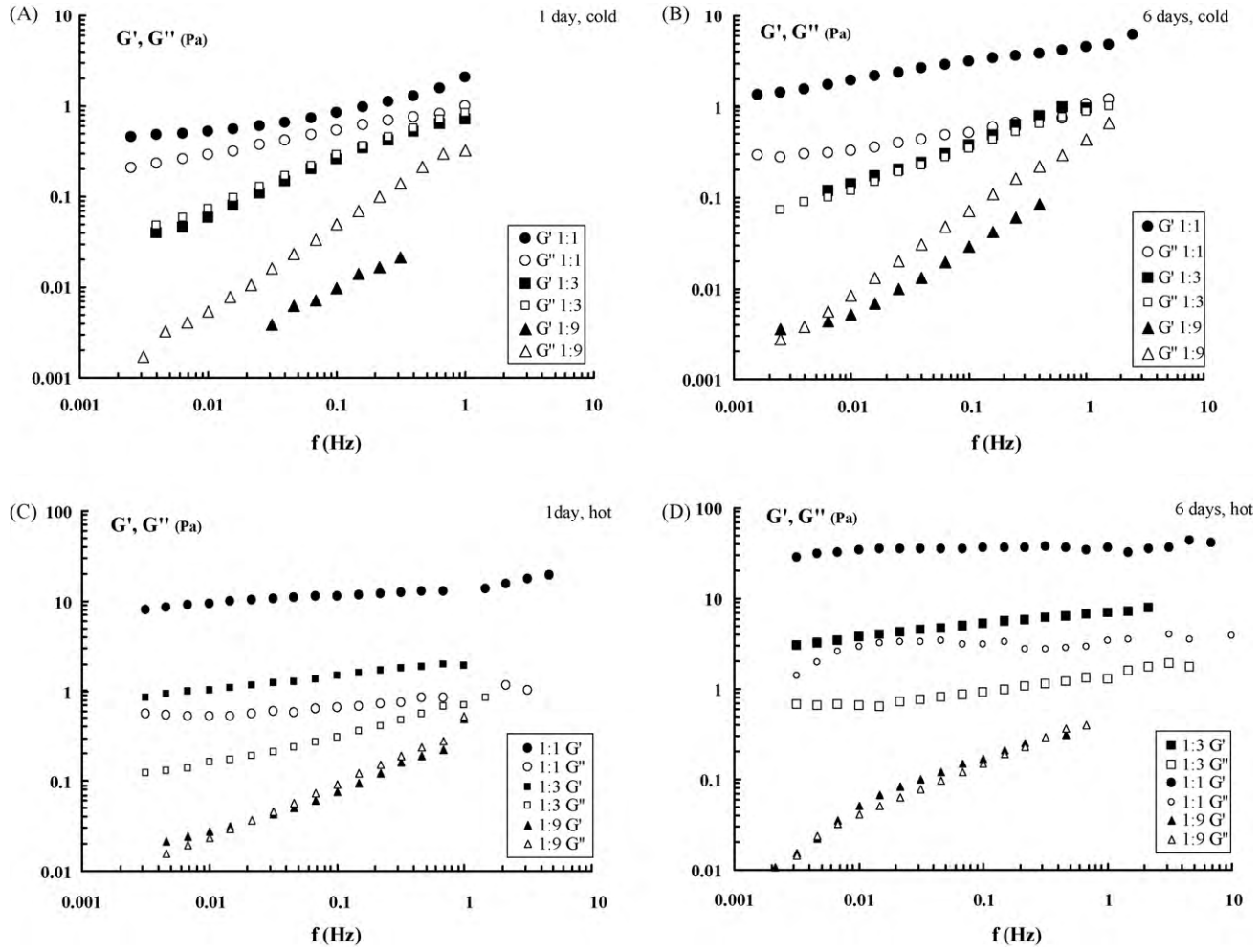

Fig. 1. Comparison among the mechanical spectra of LBG/xanthan samples prepared at different weight ratios (1:1, 1:3 and 1:9), prepared at two different temperatures (A and B: $T = 25\,^{\circ}C$; C and D: $T = 75\,^{\circ}C$) and recorded at 25 °C 1 day (A and C) and 6 days (B and D) after the preparation.

registered for the 1:3 "cold sample", Fig. 2(B)) the corresponding 1:9 "cold sample" still shows mechanical spectra typical of solutions after 6 days (Fig. 2(C)). Clearly in the 1:9 "hot sample" the Xanthan chains, being in the disordered conformation, are more capable to form physical entanglements with the LBG chains in comparison with the 1:9 "cold sample" where the solution behaviour is always observed (Fig. 2(C)). When a lower amount of Xanthan is present (1:3 ratio), for the "hot samples" (Fig. 2(E)) the evolution of a very weak gel is monitored with time, while, for the "cold samples", a gel point transition is always observed (Fig. 2(B)).

Summarizing: the variations with time of the moduli are more significant in "hot samples" (Fig. 2(D–F)). For the "cold samples" weak gel behaviour is monitored for the 1:1 ratio while gel behaviour is monitored for the corresponding "hot samples" (Fig. 2(A) and (D)). The 1:9 ratio "hot samples" show a gel point transition with a negligible evolution with time while, for the "cold samples", the corresponding spectra are those typical of solutions (Fig. 2(C) and (F)). For the 1:3 ratio the "hot samples" are weak gels while the "cold samples" are at the gel point (Fig. 2(B) and (E)).

The 1:1 ratio is the most effective leading to a gel for both temperature preparation conditions (tough weak gel is formed in the case of the "cold samples"). The difference detected between the 1:3 (gel point for the "cold samples") and 1:9 ratios (gel point for the "hot samples"), indicates the crucial role played by the conformation of the Xanthan chains. When a high amount of Xanthan chains is present in double helix conformation (1:9, "cold samples"), a predominant liquid-like behaviour is observed. On the other side, when the Xanthan chains are in the disordered conformation, also for a high amount of the polysaccharide (1:9, "hot samples"), a gel point transition is monitored.

It is interesting to point out that the critical exponents for gelation, n, are very close to the theoretical one 0.5 (Chambon, Petrovic, MacKnight, & Winter, 1986) for both 1:3, "cold samples" and 1:9, "hot samples" (Table 1), i.e., for those samples showing a gel point behaviour.

Actually such theoretical 0.5 value was firstly hypothesized by Winter and Chambon (1986) as the universal parameter for the sol–gel transition, nevertheless later works clarified that there is no universal value for n that can assume any value between 0 and 1, depending on several parameters, such as cross-linker amount, polymer concentration, molecular weight, and the specific pre-gel history (Coviello & Burchard, 1992; Grisel & Muller, 1998; Hsu & Jamieson, 1993; Matricardi, Dentini, Crescenzi, 1993; Michon, Cuvelier, & Launay, 1993; Richter, Boyko, & Schröter, 2004; Richter, Boyko, Matzker, & Schröter, 2004; Sandolo, Matricardi, Alhaique, & Coviello, 2009; Winter, Izuka, & De Rosa, 1994). Usually, in a cross-linking reaction, just beyond the gel point, G' levels off as the frequency decreases, and G'' is proportional to ω. At later stages of the reaction, the equilibrium modulus increases and G' and G'' depart from each other. This is actually what we observe for our "cold samples" at different weight ratios: the solution behaviour for the 1:9, the gel point behaviour for the 1:3 and the gel behaviour for the 1:1 samples (Fig. 1(B)). In the case of "hot samples" the solution behaviour is not detectable but gel point, weak gel and

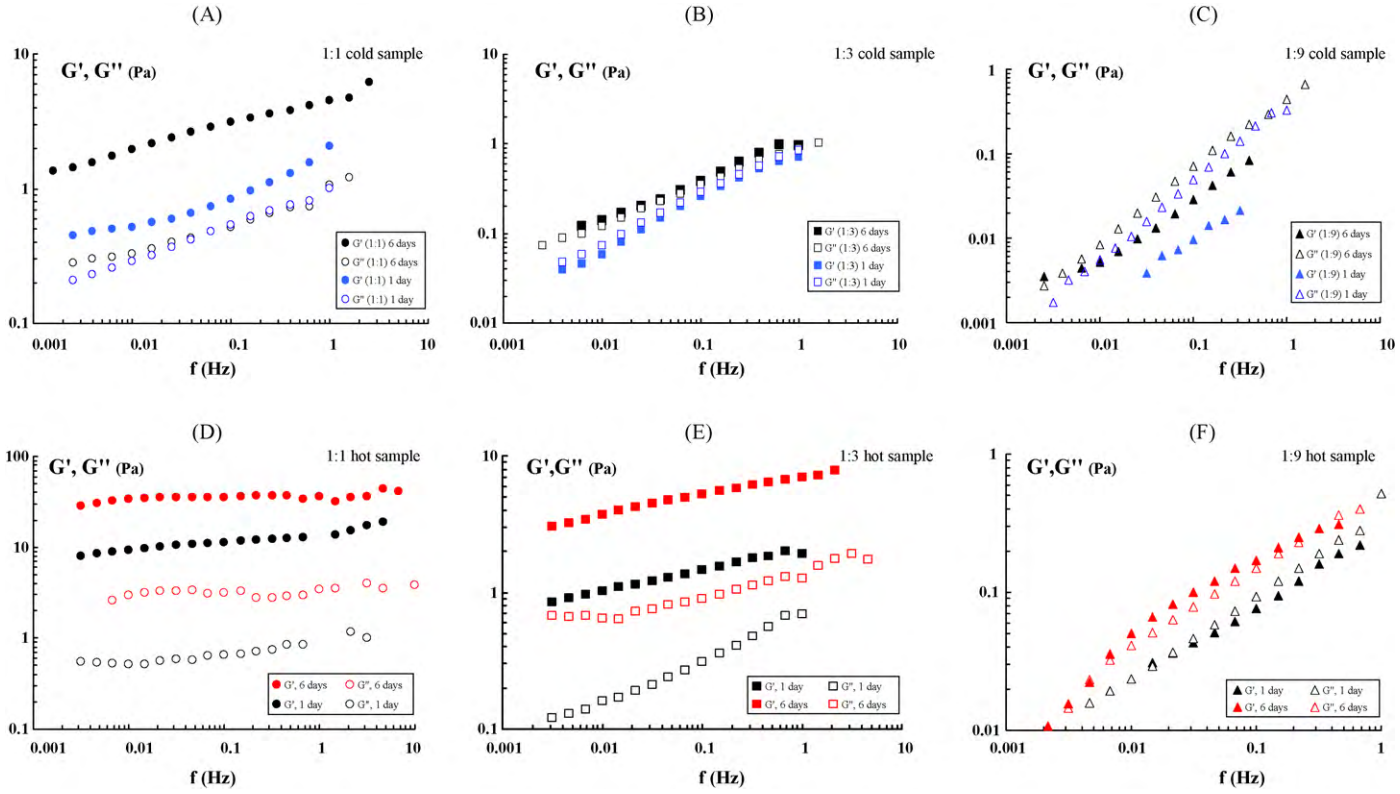

Fig. 2. Comparison among the mechanical spectra of LBG/xanthan recorded at 25 °C 1 day and 6 days after the preparation at different weight ratios. "Cold samples": A: 1:1; B: 1:3 and C: 1:9. "Hot samples": D: 1:1; E: 1:3 and F: 1:9.

gel behaviours are monitored for the 1:9, for the 1:3 and for 1:1 samples, respectively (Fig. 1(D)).

The critical exponent value of 0.5 detected for the two cases above reported (1:9 "hot samples" and 1:3 "cold samples") suggests that, in accordance with the critical exponent found for stoichiometric chemical cross-linkings, the networks are based on "one to one" interactions between the LBG and Xanthan chains. In the case of the 1:9 "cold sample" there are actually too few LBG chains able to build up a three-dimensional network (Fig. 2(C)). As LBG increases (1:3 "cold sample") a gel point is observed indicating that a sufficient number of LBG chains can interact with Xanthan (Fig. 2(B)). Finally, for the 1:1 "cold sample" a real weak gel is obtained (Fig. 2(A)). In conclusion it can be assumed that, for the "cold samples", the network is mainly dominated by LBG and the network formation is mediated by the addition of an appropriate amount of Xanthan chains. Furthermore, the usual evolution with time of the two moduli (and correspondingly of the mechanical spectra) observed for a chemical cross-linking reaction, is detected here by changing the weight ratio between the two polymers (Fig. 1(B)).

A quite different situation occurs for the "hot samples": at 75 °C LBG keeps its random coil conformation (present at room temperature) but also Xanthan is dispersed as single chains. Actually, Xanthan is not allowed to renaturate during cooling, because it is implied in the network formation with the LBG chains. In this case no solution behaviour is ever detected: the 1:9 "hot sample" is already at the gel point (Fig. 2(F)), thus showing that the different conformations assumed by Xanthan play a crucial role in the building up of the network. For the other ratios, 1:3 and 1:1, weak gel and gel behaviours are monitored (Fig. 2(E) and (D)).

For the LBG/Xanthan cross-linking reaction it is also possible to assume an analogy between the weight ratio and the reaction time and to report the loss tangent ($tan\,\delta$) as a function of the weight ratio (instead of the reaction time). In fact, according to the definition of the gel point the loss tangent is given (Kramers–Kronig relation) by $tan\,\delta = tan(n\pi/2) = G''/G'$ (Ferry, 1980), indicating that $tan\,\delta$, at the sol–gel transition, is independent on ω and its value depends only on n. Fig. 3(A) shows the results obtained by dynamic frequency sweep measurements for some selected ratios (1:9, 1:3 and 1:1 "cold samples") by plotting $tan\,\delta$ measured at various frequencies as a function of the LBG weight ratio. According to the Winter–Chambon criterion (Winter, Morganelli, & Chambon, 1988) the weight ratio at which $tan\,\delta$ curves converge is defined as the gel point. For the samples, prepared in "cold conditions", this value is

Table 1
Apparent exponents relative to the two moduli, n' and n'', evaluated for two weight ratios, power law exponents from the TCFs and the corresponding fractal dimensions, d_f.

	Rheology				Light scattering	
	"Cold samples" (1:3)		"Hot samples" (1:9)		"Cold samples" (1:3)	"Hot samples" (1:9)
Time (days)	n'	n''	n'	n''	μ	μ
1	0.56	0.54	0.53	0.59		
6	0.47	0.43	0.50	0.56	0.48	0.44
Time (days)	d_f (n')	d_f (n'')	d_f (n')	d_f (n'')	d_f	d_f
1	1.92	1.95	1.96	1.89		
6	2.04	2.08	2.00	1.93	2.08	2.27

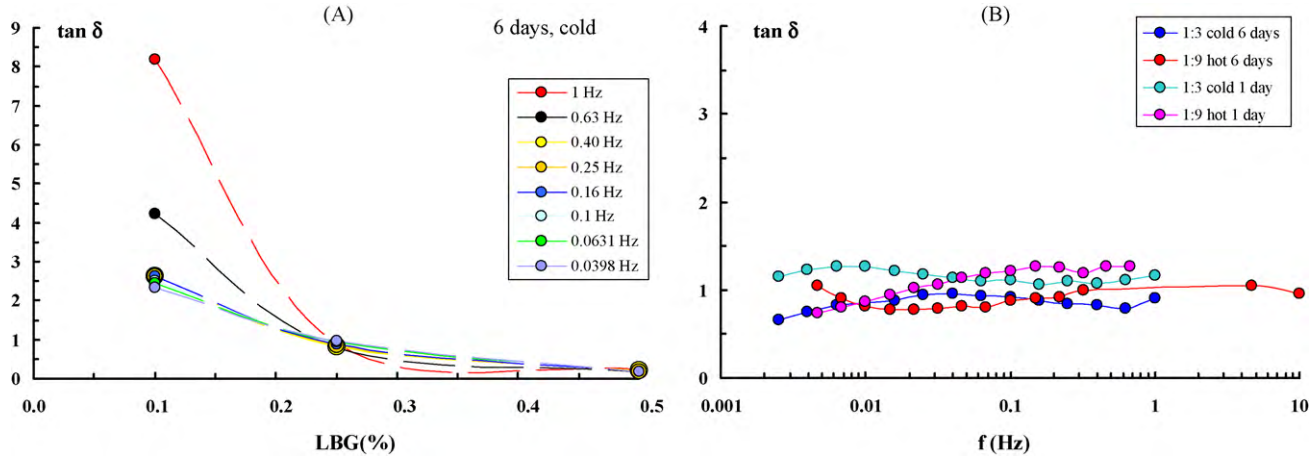

Fig. 3. (A) Tan δ of LBG/xanthan samples prepared in "cold conditions" and recorded at 25 °C 6 days after the preparation at different frequencies as a function of the content of LBG (e.g., LBG = 0.50 corresponds to 1:1 weight ratio). (B) Tan δ of LBG/xanthan samples prepared in "hot" and "cold conditions" as a function of frequency for the 1:3 and 1:9 ratios.

practically coincident with the 1:3 weight ratio and is equal to 1. The frequency-dependent measurement at the gel point should exhibit the same slope for G' and G'', as shown in Fig. 1(B) and reported in Table 1. Thus, for the LBG/Xanthan weight ratios corresponding to the gel point, 1:3 "cold sample" and 1:9 "hot sample", $tan\,\delta \approx 1$ (and therefore $n \approx 0.5$), as shown in Fig. 3(B), for both systems, in the whole explored frequency domain.

Furthermore, the power law observed at the gel point implies a selfsimilar structure of the network (Muthukumar, 1985; Vilgis & Winter, 1988); thus, it can be assumed that also the LBG/Xanthan networks assume a selfsimilar structure when the gel point is detected (1:3 "cold sample" and 1:9 "hot sample"), and such connectivity can be related to the fractal dimension, d_f. In fact, according to an important, and still valid work (Muthukumar, 1989), in the case that the excluded volume effect is fully screened the following relation holds for a polydisperse system: $n = d(d+2-2d_f)/2(d+2-d_f)$, where d is the space dimension (i.e., 3). For the tested systems (see Table 1) at the gel point (1:3 "cold sample" and "1:9 "hot sample") $n \approx 0.5$ and the corresponding d_f value is ≈2, the same of an isolated linear chain of infinite length under θ conditions (Muller, Gérard, Dugand, Rempp, & Gnanou, 1991). This d_f value could be surprising for a chemical cross-linking reaction where at the gel point the polymer is a highly branched macromolecule, but it can be reasonable for a physical gel. In this case the critical state is not due to the simultaneous chemical reaction of many monomers, but to the physical interactions among chains of quite long contour length (order of hundred of nm). As a consequence the build up of peculiar structures is observed, as those typical of biological networks that rarely can be strictly identified within the theoretical frameworks of electrical analogue or tree-models.

3.2. Light scattering investigations

The intensity autocorrelation functions (TCF) of LBG/Xanthan samples prepared at the three different weight ratios in "hot" and "cold conditions", were acquired 6 days after the preparation. DLS measurements were carried out by collecting the signal on different regions of each sample to take into account the non-ergodicity of gel systems. Results are shown in Fig. 4. Samples with a higher content of LBG display higher values of a no-decay component, which is an indication of the presence of a higher fraction of scattered light coming from scatterers unable to relax over the applied experimental time scale. For a given weight ratio of LBG/Xanthan, "hot samples" appear always more dynamically frozen than the cold ones. By comparing the time dependence of TCFs it can be noted that the dynamics of samples 1:1, either "hot" or "cold", and 1:3 "hot", appears to be almost entirely frozen, whereas the autocorrelation function of sample 1:9 "cold" displays a liquid-like character. Furthermore, samples 1:3 "cold" and 1:9 "hot" follow a power-law dependence, $g^{(2)} \approx t^{-\mu}$, with an exponent μ of 0.48 and 0.44, respectively. This power law behaviour is usually taken as a mark of the gelation threshold (Shibayama & Norisuye, 2002). The same two samples were seen to be at the gelation point with a critical exponent close to 0.5 by rheological results (see Section 3.1). Although a relation between critical exponents obtained by DLS and rheology is predicted by the Doi and Onuki theory (Richter, 2007), the critical exponents obtained by means of light scattering measurements were, in the present study, lower than those derived by rheology, as already observed by other researchers for several different systems (Richter, 2007).

The dynamic properties of the samples were also investigated by looking at the statistical properties of the scattered light. Indeed, gel systems are characterized by the presence of very slow fluctuations in the average intensity reflecting the reduced speckle mobility (Rodd et al., 2001) and due to either dynamical or structural network inhomogeneities (Richert, 2002). For each scattering angle the intensity from single speckles was collected with an integration time of 1 s over different sample positions. Data were then normalized by their mean value and the data distribution was fitted to the convolution of a Gaussian with an exponential function

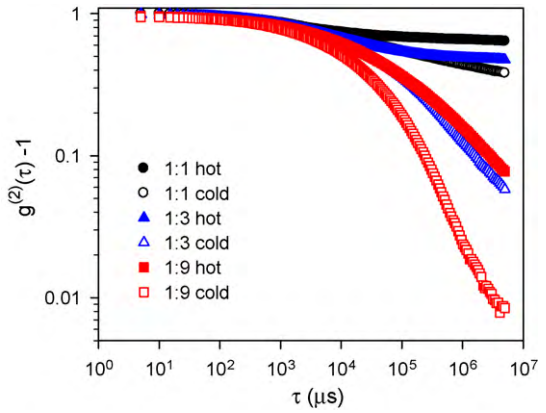

Fig. 4. Intensity autocorrelation functions of LBG/xanthan samples obtained 6 days after their preparation.

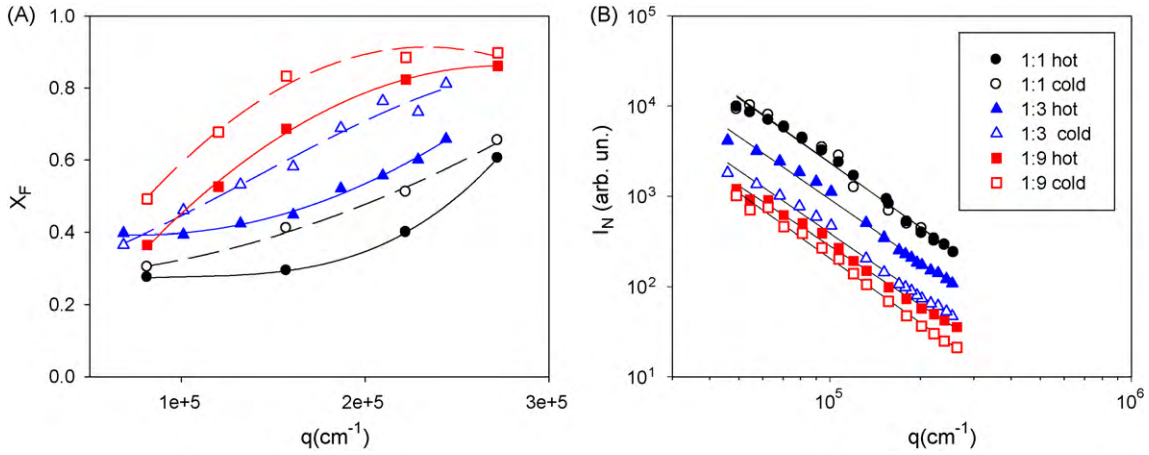

Fig. 5. Fraction of the fast relaxing contribution to scattered light vs. wave-vector q estimated for the LBG/xanthan studied at different weight ratios (A). Log–log plot of the average scattered light intensity, measured for the LBG/xanthan at different weight ratios, vs. q-vector. Data were normalized by toluene scattering and the weight average molecular weight (B).

(see Eq. (1)), which allowed to distinguish the fast fluctuating and slowly relaxing contribution. The fraction of the fast contribution to the scattered light at different q-vector values is shown in Fig. 5(A). A lower fraction of the fast relaxing contribution, X_F, is observed at higher LBG content, with the "hot samples" being more frozen than the "cold" ones, consistently with the DLS results. The decrease of X_F with q lowering implies that density fluctuations occurring over larger length scale are more hindered. This was observed in all samples, including LBG 1:9 "cold", that appears liquid in the range of several ten nanometers.

Information on the structural properties can be provided by the dependence of the scattered light intensity on q wave-vector.

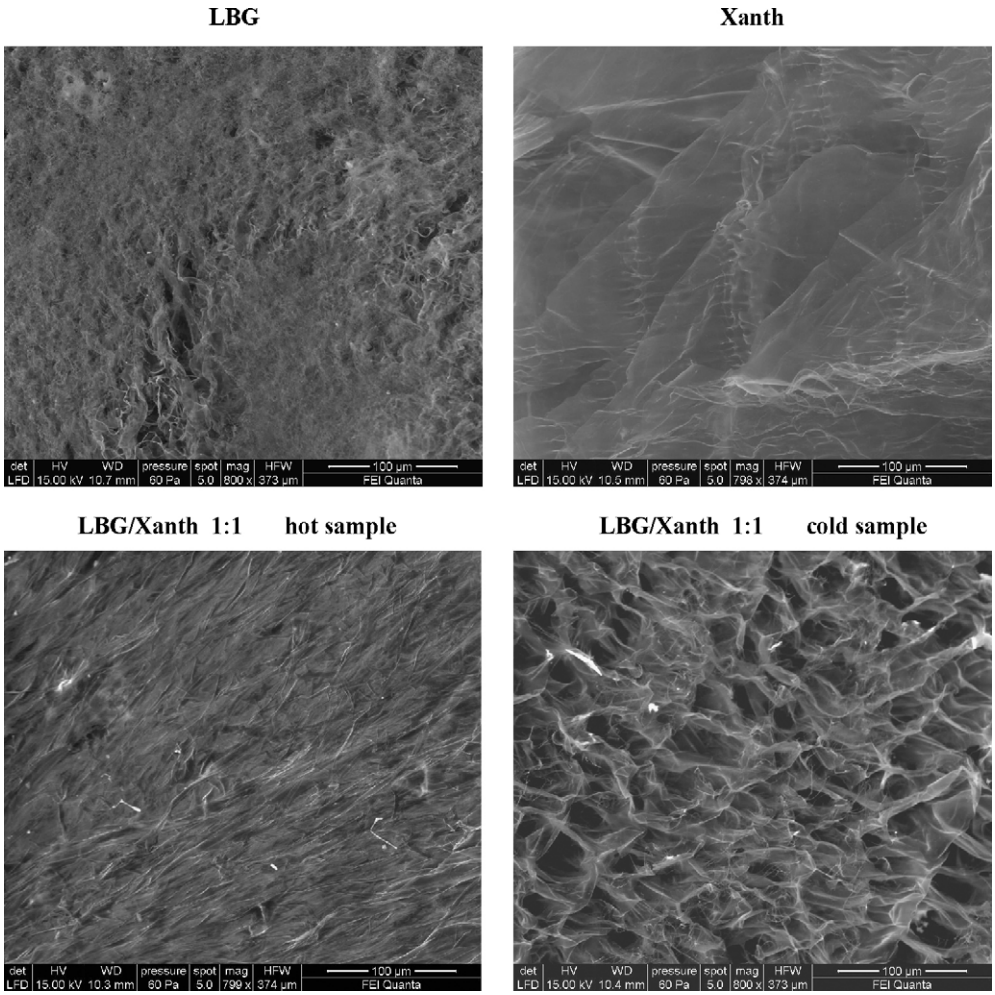

Fig. 6. Scanning electron micrograph of surface morphology of freeze-dried samples of LBG, xanthan (top), and LBG/xanthan 1:1 (bottom) prepared at 75 and 25 °C (magnification 800×).

Indeed, for a system of molecules in solution, the q-dependence of the scattered light is given by:

$$I(q) \propto P(q)S(q)$$

where $P(q)$ is the form factor of the single molecule and $S(q)$ is the structure factor giving the intensity contribution due to the spatial correlation between molecules in solution. In the case of fractal aggregates, $S(q)$ follows a power-law (Thill et al., 2000) of the form $S(q) \propto q^{-d_f}$. The law is valid only over a length scale smaller than the aggregate dimension (R) and larger than the dimension of the primary particles assembled in the aggregate (r_0), where $P(q) \approx 1$. This leads to the well known relation $I(q) \propto q^{-d_f}$ with $r_0 \ll 1/q \ll R$ often used for determining the fractal dimension. The q-dependence of the scattered intensities for LBG/Xanthan samples was obtained by averaging the signal over different regions of the sample. Data for each sample, normalized for the weight average molecular weight, are shown in Fig. 5(B).

Except for the absolute value, all samples display a very similar $I(q)$ profile, despite their different dynamical behaviours. A sign of curvature can be envied in $S(q)$ profile at about $6 \times 10^4\ \mathrm{cm}^{-1}$ (corresponding to 170 nm) that could signal the approaching to some characteristic length of the system. At higher q values, $I(q)$ follows a power-law with a slope of 2.4 ± 0.2. This value of fractal dimension indicates a selfsimilar and quite compact structure, somehow larger, but anyhow comparable, than that obtained from rheology and DLS for samples 1:3 "cold" and 1:9 "hot". However, sample polydispersity may severely affect the accuracy of the fractal dimension determination by means of this type of data, since aggregates of different sizes can contribute to scattered intensity with a different form factor. The similarity of $I(q)$ profile for the different samples suggests that the structure is almost the same, at least on the length scale ranging from two hundred down to few nanometers. A further comment can be made on the variation of the intensity absolute value for the different samples. Actually, we observe that the intensity increases with the increase of LBG content in the samples and the increase is even higher for those systems behaving as "strong" gels, although the average spatial coordination inside the aggregates does not appreciably change, suggesting the formation of ticker or denser junction regions inside the same type of aggregates.

3.3. Scanning electron microscopy characterization

The SEM micrographs, taken 6 days after preparation on freeze-dried samples, support the considerations above discussed. In Fig. 6 the photographs of the two single polymers (LBG and Xanthan) and of the two samples prepared at low and high temperature with a weight ratio of 1:1 are shown. The last two systems are both gels, as indicated by the frequency spectra and by the TCFs, but the different strengths of the networks, estimated with the absolute values of the elastic moduli and by the decay behaviour of the two TCFs, is clearly evidenced by the different textures observed in the pictures.

It is interesting to appreciate the variations between the initial aspect of the single polymers, and the final situations, when the synergistic effects, deeply influenced by the preparation temperature, change dramatically also the macroscopic morphology of the mixed systems.

4. Conclusions

The LBG/Xanthan system leads to different types of network depending on the ratio of the two polymers and on the preparation temperature. In particular, for the 1:1 ratio a gel is always obtained; for the 1:3 ratio a weak gel is observed in "hot conditions" while a gel point is detected in "cold conditions"; for the 1:9 ratio the gel point is monitored in "hot conditions" while the solution is present in "cold conditions". These results indicate how a fine tuning of the properties of the mixed gels is possible through the variation of the preparation temperature and/or the weight ratio between the two polymers.

Interesting is the qualitative agreement between the two approaches: the TCFs of 1:1 samples ("hot" and "cold" samples) do not relax in the explored time window and similarly the corresponding mechanical spectra are those of a gel in the whole explored frequency domain. Also for the other two weight ratios a correspondence between the rheology and the DLS can be appreciated.

Furthermore, looking at the values of Table 1, it is possible to see the good accordance between the fractal dimensions, obtained with the rheology approach, and the DLS technique for the two systems that show sol–gel transition in the mechanical spectra and power law behaviour in DLS.

The slight discrepancy between the two critical exponents is reasonable: the theory mainly deals with chemical network formation while in the present case physical interactions lead to the gel: furthermore, the light scattering is a non-perturbative technique while a periodic deformation is applied in rheology partly disturbing the cross-linking process with a possible shift in the determination of the infinite cluster formation and detection.

Acknowledgements

Financial support from FIRB, Fondo per gli Investimenti della Ricerca di Base, Research Program: Ricerca e Sviluppo del Farmaco (CHEM-PROFARMA-NET), grant no. RBPR05NWWC_003 is acknowledged.

References

Baichwal, A. R. (2004). Sustained-release matrix for high-dose insoluble drugs. *US Patent Office*, Pat. No. 2,004,121,012.

Barthès, J., Bulone, D., Manno, M., Martorana, V., & San Biagio, P. L. (2007). A statistical light scattering approach to separating fast and slow dynamics. *European Biophysical Journal*, *36*, 743–752.

Cairns, P., Miles, M. J., Morris, V. J., & Brownsey, G. J. (1988). X-ray fibre-diffraction studies of synergistic, binary polysaccharide gels. *Carbohydrate Research*, *176*, 329–334.

Chambon, F., Petrovic, Z. S., MacKnight, W. J., & Winter, H. H. (1986). Rheology of model polyurethanes at the gel point. *Macromolecules*, *19*, 2146–2149.

Coviello, T., & Burchard, W. (1992). Criteria for the point of gelation in reversibly gelling systems according to dynamic light scattering and oscillatory rheology. *Macromolecules*, *25*, 1011–1012.

Coviello, T., Kajiwara, K., Burchard, W., Dentini, M., & Crescenzi, V. (1986). Solution properties of xanthan. 1. Dynamic and static light scattering from native and modified xanthans in dilute solutions. *Macromolecules*, *19*, 2826–2831.

Dea, I. C. M., Clark, A. H., & McCleary, B. V. (1986). Effect of galactose-substitution-patterns on the interaction properties of galactomannans. *Carbohydrate Research*, *147*, 275–294.

Dolz, M., Hernández, Delegido, J., Alfaro, M. C., & Muñoz, J. (2007). Influence of xanthan gum and locust bean gum upon flow and thixotropic behaviour of food emulsions containing modified starch. *Journal of Food Engineering*, *81*, 179–186.

Fadden, D. J., Kulkarni, N. M., & Sorg, A. F. (2004). Fast dissolving orally consumable films containing a modified starch for improved heat moisture resistance. *US Patent Office*, Pat. No. 2,004,247,648.

Ferry, J. D. (1980). *Viscoelastic properties of polymers* (3rd ed.). New York: Wiley.

Grisel, M., & Muller, G. (1998). Rheological properties of the schizophyllan–borax system. *Macromolecules*, *31*, 4277–4281.

Hacche, L. S., Washington, G. E., & Brant, D. A. (1987). Light-scattering investigation of the temperature-driven conformation change in xanthan. *Macromolecules*, *20*, 2179–2187.

Hsu, S. H., & Jamieson, M. (1993). Viscoelastic behaviour at the thermal sol–gel transition of gelatin. *Polymer*, *34*, 2602–2608.

Kok, M. S., Hill, S. E., & Mitchell, J. R. (1999). Viscosity of galactomannans during high temperature processing: Influence of degradation and solubilisation. *Food Hydrocolloids*, *13*, 535–542.

Lapasin, R., & Pricl, S. (1995). *Rheology of industrial polysaccharides: Theory and applications*. London: Blackie Academic & Professional.

Lundin, L., & Hermansson, A. M. (1995). Supermolecular aspects of xanthan–locust bean gum gels based on rheology and electron microscopy. *Carbohydrate Polymers*, *26*, 129–140.

Mandala, I., Kapetanakou, A., & Kostaropoulos, A. (2008). Physical properties of breads containing hydrocolloids stored at low temperature. II. Effect of freezing. *Food Hydrocolloids*, *22*, 1443–1451.

Mannion, R. O., Melia, C. D., Mitchell, J. R., Harding, S. E., & Green, A. P. (1991). Effect of xanthan/locust bean gum synergy on ibuprofen release from hydrophilic matrix tablets. *Journal of Pharmacy and Pharmacology, Supplement*, *43*, 79P–79P.

Manno, M., Bulone, D., Martorana, V., & San Biagio, P. L. (2004). Ergodic to non-ergodic transition monitored by scattered light intensity statistics. *Physica A*, *341*, 40–54.

Matricardi, P., Dentini, M., & Crescenzi, V. (1993). Rheological gel-point determination for a polysaccharide system undergoing chemical cross-linking. *Macromolecules*, *26*, 4386–4387.

Michon, C., Cuvelier, G., & Launay, B. (1993). Concentration dependence of the critical viscoelastic properties of gelatin at the gel point. *Rheologica Acta*, *32*, 94–103.

Morris, E. R. (1990). Mixed polymer gels. In P. Harris (Ed.), *Food gels* (pp. 291–359). London, UK: Elsevier.

Muller, R., Gérard, E., Dugand, P., Rempp, P., & Gnanou, Y. (1991). Rheological characterization of the gel point: A new interpretation. *Macromolecules*, *24*, 1321–1326.

Muthukumar, M. (1985). Dynamics of polymeric fractals. *Journal of Chemical Physics*, *83*, 3161–3166.

Muthukumar, M. (1989). Screening effect on viscoelasticity near the gel point. *Macromolecules*, *22*, 4656–4658.

Ojinnaka, C., Brownsey, J. G., Morris, E. R., & Morris, V. J. (1998). Effect of deacetylation on the synergistic interaction of acetan with locust bean gum or konjac mannan. *Carbohydrate Research*, *305*, 101–108.

Pedersen, J. K. (1980). Carrageenan, pectin and xanthan/locust bean gum gels. Trends in their food use. *Food Chemistry*, *6*, 77–88.

Pusey, P., & van Megen, W. (1989). Dynamic light scattering by non-ergodic media. *Physica A*, *157*, 705–741.

Ramírez, J. A., Barrera, M., Morales, O. G., & Vázquez, M. (2002). Effect of xanthan and locust bean gums on the gelling properties of myofibrillar protein. *Food Hydrocolloids*, *16*, 11–16.

Richert, R. (2002). Heterogeneous dynamics in liquids: Fluctuations in space and time. *Journal of Physics: Condensed Matter*, *14*, R703–R738.

Richter, S. (2007). Comparison of critical exponents determined by rheology and dynamic light scattering on irreversible and reversible gelling systems. *Macromolecular Symposia*, *256*, 88–94.

Richter, S., Boyko, V., Matzker, R., & Schröter, K. (2004). Gelation studies: Comparison of the critical exponents obtained by dynamic light scattering and rheology, 2^a A thermoreversible gelling system: Mixtures of xanthan gum locust bean gum. *Macromolecular Rapid Communication*, *25*, 1504–1509.

Richter, S., Boyko, V., & Schröter, K. (2004). Gelation studies on a radical chain cross-linking copolymerization process: Comparison of the critical exponents obtained by dynamic light scattering and rheology. *Macromolecular Rapid Communication*, *25*, 542–546.

Richter, S., Brand, T., & Berger, S. (2005). Comparative monitoring of the gelation process of a thermoreversible gelling system made of xanthan gum and locust bean gum by dynamic light scattering and ^{1}H NMR spectroscopy. *Macromolecular Rapid Communication*, *26*, 548–553.

Rodd, A. B., Dunstan, D. E., Boger, D. V., Schmidt, J., & Burchard, W. (2001). Heterodyne and nonergodic approach to dynamic light scattering of polymer gels: Aqueous xanthan in the presence of metal ions (aluminum(III)). *Macromolecule*, *34*, 3339–3352.

Rolf, D. (2003). Aqueous gel wound dressing and package. *US Patent Office*, Pat. No. 6,620,436.

Sahin, H., & Ozdemir, F. (2004). Effect of some hydrocolloids on the rheological properties of different formulated ketchups. *Food Hydrocolloids*, *18*, 1015–1022.

Sandolo, C., Matricardi, P., Alhaique, F., & Coviello, T. (2009). Effect of temperature and cross-linking density on rheology of chemical cross-linked guar gum at the gel point. *Food Hydrocolloids*, *23*, 210–220.

Secouard, S., Malhiac, C., Grisel, M., & Decroix, B. (2003). Release of limonene from polysaccharide matrices: Viscosity and synergy effect. *Food Chemistry*, *82*, 2227–2234.

Shibayama, M., & Norisuye, T. (2002). Gel formation analyses by dynamic light scattering. *Bulletin of the Chemical Society of Japan*, *75*, 641–659.

Sugden, K. (1989). Buccal etorphine tablets with xanthan and locust bean gums. *US Patent Office*, Pat. No. 4,829,056.

Thill, A., Lambert, S., Moustier, S., Ginestet, P., Audic, J. M., & Bottero, J. Y. (2000). Structural interpretations of static light scattering patterns of fractal aggregates. *Journal of Colloid and Interface Science*, *228*, 386–392.

Ughini, F., Andreazza, I. F., Ganter, J. L. M. S., & Bresolin, T. M. B. (2004). Evaluation of xanthan and highly substituted galactomannan from *M. scabrella* as a sustained release matrix. *International Journal of Pharmaceutics*, *271*, 197–205.

Venkataraju, M. P., Gowda, D. V., Rajesh, K. S., & Shivakumar, H. G. (2008). Xanthan and locust bean gum (from *Ceratonia siliqua*) matrix tablets for oral controlled delivery of metoprolol tartrate. *Current Drug Therapy*, *3*, 70–77.

Vilgis, T. A., & Winter, H. H. (1988). Mechanical selfsimilarity of polymers during chemical gelation. *Colloid and Polymer Science*, *266*, 494–500.

Wang, E., Wang, Y. J., & Sun, Z. (2002). Conformational role of xanthan in its interaction with locust bean gum. *Journal of Food Science*, *67*, 2609–2614.

Winter, H. H., & Chambon, F. (1986). Analysis of linear viscoelasticity of a crosslinking polymer at the gel point. *Journal of Rheology*, *30*, 367–382.

Winter, H. H., Morganelli, P., & Chambon, F. (1988). Stoichiometry effects on rheology of model polyurethanes at the gel point. *Macromolecules*, *21*, 532–535.

Winter, H. H., Izuka, A., & De Rosa, M. E. (1994). Experimental observation of the molecular weight dependence of the critical exponents for the rheology near the gel point. *Polymer Gels and Networks*, *2*, 239–245.

Zhan, D. F., Ridout, M. J., Brownsey, G. J., & Morris, V. J. (1993). Xanthan–locust bean gum interactions and gelation. *Carbohydrate Polymers*, *21*, 53–58.